Eur. Phys. J. A **3**, 93–98 (1998)

THE EUROPEAN PHYSICAL JOURNAL A

Limitations of modulation analysis for dark matter direct detection experiments

Y. Ramachers[a], M. Hirsch[b], H.V. Klapdor–Kleingrothaus[c]

Max–Planck–Institut für Kernphysik, P.O.Box 10 39 80, D–69029 Heidelberg, Germany

Received: 22 May 1998
Communicated by B. Povh

Abstract. We examine the limitations of the data analysis scheme for annual modulations as a signature of WIMP direct detection. The consequences for existing and planned experiments are pointed out. These include determinations of optimum recoil energy regions to be analyzed for modulations and the minimum target mass needed to detect them. Calculations for ^{23}Na, nat. Ge, and ^{129}Xe as example nuclei have been performed.

PACS. 95.35 Dark Matter

1 Introduction

Direct detection experiments looking for WIMPs (Weakly Interacting Massive Particles) as constituents of the dark matter in our galaxy can follow two different search strategies: First (and usually done up to now), experiments can give limits for cross sections of unknown WIMPs as function of their mass [1–3].

Second, experiments can look for a distinctive WIMP signature, *e.g.* modulations of the supposed WIMP–spectrum in time. Most prominent is the annual modulation mechanism caused by the movement of the earth around the Sun [4,5]. While the Sun circulates around the galactic center, the orbital speed of the Earth around the Sun induces a periodic modulation of velocities of WIMPs reaching the Earth. This modulation of kinetic energies of WIMPs can in principle be detected and hence is a signature for WIMP direct detection. Other periodic signatures are diurnal modulations [6,7] and annual modulations due to the Suns gravitational focusing of WIMPs entering the solar system [8] (these are orthogonal to the annual velocity variations). All these signatures require essentially the same data analysis scheme, adopting different amplitudes, frequencies and/or phases. Therefore we concentrate on modulations induced by the annual velocity variations as signature for WIMP detection. The limitations of the statistical data analysis scheme for detection of this signature are the subject of this article.

The foundations for our analysis have been laid about ten years ago [5], nowadays experiments are performed to find the WIMP signature [9]. We found it worthwhile to extend the statistical analysis scheme and point out consequences. The importance of WIMP signature searches to obtain more detailed information about WIMPs is stressed in [10].

[a] E-mail: yorck@mickey.mpi-hd.mpg.de
[b] E-mail: mahirsch@mickey.mpi-hd.mpg.de
[c] E-mail:klapdor@mickey.mpi-hd.mpg.de
Correspondence to: Y. Ramachers

2 Limitations of the modulation analysis

Following [5] one can analyze a time series of count rates binned in days as consisting of two different parts (time-dependent signal in constant noise):

$$D\,(t) - \langle B\rangle = \underbrace{\langle S\rangle}_{const.\ signal} + \underbrace{S_m\,\cos(\omega\,t)}_{periodic\ signature}\ , \qquad (1)$$

where brackets mean the average of the Poisson distributed variables, D is the count rate per day in a given detector, ω is the inverse annual period and S_m the modulation amplitude. The noise (S + B) has been subdivided into two parts since the modulation signal is superposed on a constant WIMP–signal S and an unknown but constant background B.

The time series is then transformed by a cosine transformation and one defines a new random variable X as

$$X \equiv \sum_i 2\,\cos(\omega\,t_i)\,D(t_i), \qquad (2)$$

which is normal distributed with variance $\sigma^2(X)$ and summation is over days. One then defines the modulation significance random variable $R \equiv X/\sigma(X)$ which is normal distributed with zero mean for $S_m = 0$ and unit variance. This procedure is similar to the Rayleigh test [11] for detection of weak periodic signals buried in uniform noise.

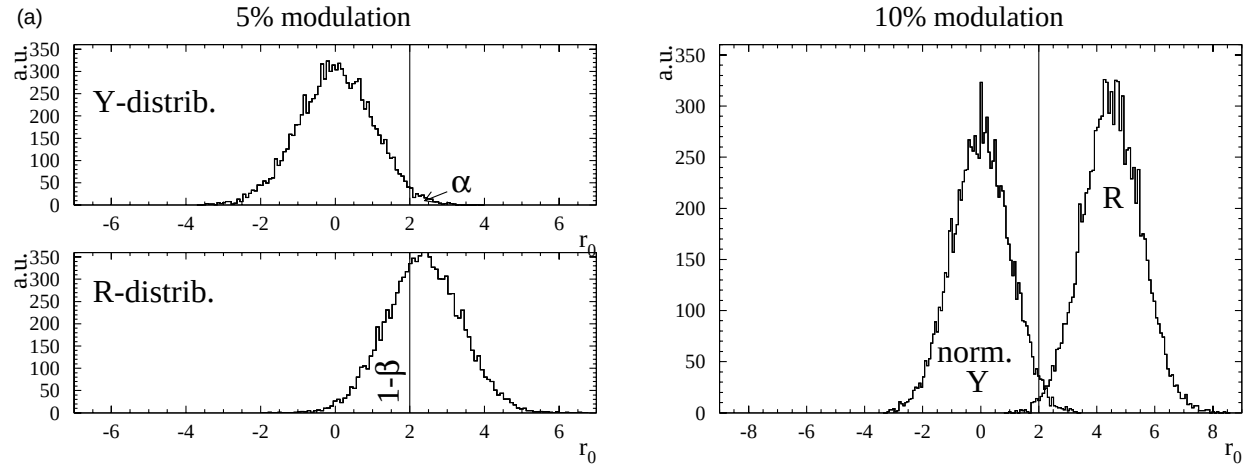

Fig. 1. Distributions for the normalized check variable and the modulation significance resulting from a simulation of 10^4 year–long experiments. From left to right with a 5% and 10% modulation, respectively. Assumed is a constant signal with 10 events per day ($\langle B\rangle = 0$). Indicated by the vertical line is the 97.5% C.L. corresponding to $r_0 = 2$. The areas corresponding to the errors of the first (α) and second ($1-\beta$) kind are shown in the 5% picture which shows the normalized Y-distribution in the top panel, the R-distribution in the lower panel. The 10% picture indicates an almost symmetric separation of the two distributions with respect to a give confidence level like we suggest to use

Due to the knowledge of the frequency and phase of the modulation one can define a random variable Y by means of an orthogonal transformation of the time series by replacing the cosine by a sine in (2). The presence of a modulation in the time series of count rates shifts the mean value $\langle R\rangle$ away from zero whereas the mean value $\langle Y\rangle$ remains at zero (compare Fig. 1).

Now one can test the hypothesis H_0: a periodic modulation exists within the measured time series, against the alternative H_1: There is no modulation in the time series. The confidence level for the statement: H_0 is true, is [5]

$$\text{C.L.} = \frac{1}{2} + \frac{1}{2}\,\text{erf}\left[\frac{r_0}{\sqrt{2}}\right], \tag{3}$$

where r_0 is the result of an analysis of a given time series D_0 for R according to (2) and $\sigma^2 = \sum_i 2\,\langle D_0(t_i)\rangle$ [5]. In [5] some values for r_0 and the corresponding confidence levels are quoted: $r_0 = 1\,(84\%),\ 2\,(97.5\%),\ 3\,(99.5\%)$.

In principle, tests for a periodic signal buried in noise do not depend on the relative magnitude of the signal amplitude to the noise level. The point is that these tests are limited for modulation analysis with low count rates. The procedure to analyze time series with low count rates has been outlined above, but we suggest a straightforward extension of [5], as explained in the following, motivated by experimental requirements.

The confidence level (3) applies to errors of the first kind, α, *i.e.* the probability that one decides H_0 to be true when in fact there is no modulation in the data. It has no significance for errors of the second kind, $1-\beta$, *i.e.* the probability to decide H_1 to be true while there is a modulation hidden in the data.

In order to visualize the situation a simulation of 10^4 measurements (one year each) has been performed. We set the mean signal rate $\langle S\rangle$ to 10 counts per day (cpd) and the mean background $\langle B\rangle$ to zero. Then two different periodic signal amplitudes were chosen corresponding to 5% and 10% modulations, respectively. The resulting distributions for the normalized check variable (unit variance) and the modulation significance are shown in Fig. 1. Once one has chosen a confidence level and the corresponding r_0 the errors of the first and second kind can be seen; the area indicated as α to the right of the cut at $r_0 = 2$ shows the error of the first kind. The area $1-\beta$, left to the cut from the R–distribution, is the error of the second kind (Fig. 1, left picture). For example, given a 5% modulation in a year–long measurement one would have a probability of nearly 50% to miss the modulation with a cut at $r_0 = 2$, i.e. the error of the second kind.

So the problem is to clearly distinguish between the two distributions to a given confidence level. We propose to demand equal confidence levels for errors of the first and second kind. Due to the symmetry of the distributions we now get

$$\langle R\rangle = 2\,r_0 \quad . \tag{4}$$

Note that this proposal is pragmatic from the point of view of designing an experiment. Following this procedure one minimizes, *e.g.* to a C.L. of 97.5%, the chance to miss the signal modulation after the tedious work of one year continuous data taking.

3 Consequences for direct detection experiments

The statistical limitations apply to pure counting experiments, *i.e.* measuring total count rates, as well as to energy–sensitive experiments, *i.e.* measuring a WIMP spectrum in recoil energy bins. Modulation analysis depends on the unknown properties of WIMPs, *e.g.* their

Table 1. Optimum recoil energy threshold ranges for total rate modulations at which the minimum masses in Fig. 4 were evaluated. The ranges follow from the variation of the dispersion velocity as stated in the text. The separated values given in the table correspond to the optimum thresholds at $\langle v^2\rangle^{1/2} = 246(323)$ km/s, respectively. Zero thresholds indicate that we calculate ideal recoil threshold energies. Their meaning is that real thresholds should be as low as possible

m_W[GeV]	$E^{thr}_{opt}(^{23}Na)$ [keV]	E^{thr}_{opt}(nat.Ge) [keV]	$E^{thr}_{opt}(^{129}Xe)$ [keV]
10	3.1;2.1	1.8;1.2	1.2;0.9
30	9.0;5.8	6.0;1.4	3.2;0.0
50	12.9;7.7	8.0;0.0	2.8;0.0
70	15.0;8.7	8.7;0.0	1.0;0.0
100	16.9;8.9	7.7;0.0	0.0;0.0
130	18.6;9.5	6.8;0.0	0.0;0.0
170	19.8;9.9	4.9;0.0	0.0;0.0
200	19.9;10.0	3.2;0.0	0.0;0.0
250	20.9;10.0	2.5;0.0	0.0;0.0
300	21.2;10.0	1.0;0.0	0.0;0.0
500	22.2;10.7	0.0;0.0	0.0;0.0
1000	22.9;10.8	0.0;0.0	0.0;0.0

mass and cross sections, which determine the expected rates. Therefore we provide examples for some WIMP masses and assume a testable rate of 1 cpd/kg for these WIMPs [12]. Below we give a scaling relation to account for more realistic scenarios (e.g. of lower count rates) but also show two important effects (of background and lower rates) in Fig. 4.

Another parameter is the velocity distribution of the WIMPs in the solar vicinity. We will adopt the well–known scenario of an isothermal halo with variations of the dispersion velocity $\langle v^2\rangle^{1/2}$ in the range from 246 km/s to 323 km/s, according to [13] and thereby show the influence of this parameter. For the calculation of the WIMP differential recoil energy spectrum we took the Bessel form factor [14] and the truncated Maxwellian velocity distribution [5]. The velocity variation due to the movement of the earth is taken to be ± 15 km/s [5].

As already noted in ref. [4,5] a general feature of the modulation signature is the increasing modulation amplitude for increasing recoil energies. This effect is due to the exponential decreasing shape of the differential recoil spectrum (compare Fig. 2). It becomes most obvious near the end of two recoil energy spectra obtained for two different WIMP velocity distributions because they have different recoil energy endpoints. Combined with the decreasing differential WIMP spectrum for increasing recoil energies one can define an optimal recoil energy region for detection of modulations in the data. These have not been calculated so far. The optimization procedure consists of finding the maximum integral signal combined with a maximum modulation amplitude (for energy bin modulations, see below). The optimal thresholds (recoil energies), tabulated in Tab. 1, are meant to guide the design of experiments. Their definition and consequences of 'detuning' the detectors are given below (8). Note that these optimum thresholds are not correlated to the cross over points for two recoil spectra taken at different times (WIMP velocity distributions).

From an experimental point of view it is desirable to know the approximate target mass required to find a WIMP signature for "reasonable" WIMP rates (current limits are around 5 cpd/kg [9,15]). The argument for the definition of the optimum recoil energy is as follows: The minimum target mass, M_{min}, for an experiment results as

$$M_{min}(E_{thr}) = \frac{\langle S_{min}(E_{thr})\rangle}{\mathrm{R}_{expect}\cdot\gamma(E_{thr})}\,, \qquad (5)$$

where $\langle S_{min}(E)\rangle$ is the WIMP signal in cpd needed to overcome the statistical limitations (Sec. 2) and $\gamma(E_{thr})$ is the fraction of the total expected rate R_{expect}(in cpd/kg) above recoil threshold E_{thr}.

For a given target material, WIMP mass and halo velocity dispersion the relative modulation amplitude δ(E) and the relative fraction of the WIMP signal γ(E) can be calculated [5]:

$$\delta(E) = \left|\frac{S_m(E)}{\langle S(E)\rangle}\right| \quad ;\ \gamma(E) = \frac{\langle S(E)\rangle}{\langle S(0)\rangle}\,. \qquad (6)$$

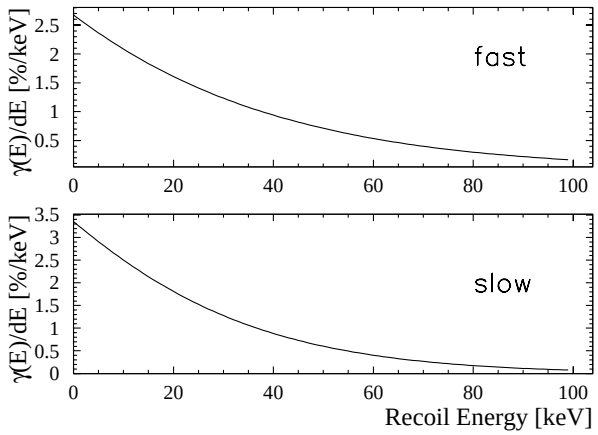

Fig. 2. Normalized WIMP–spectra as function of the recoil energy for the fast (top) and slow (bottom) WIMP halo scenario for the example of a 60 GeV WIMP scattered on ^{23}Na nuclei. The diagrams show for example the low WIMP–signal content in single keV bins as well as the general shape of a WIMP–spectrum

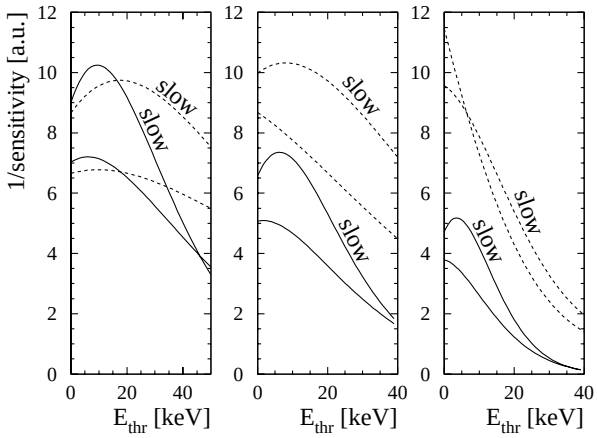

Fig. 3. The inverse mass–sensitivity (from (8)) as function of the energy threshold for two example WIMP masses, 30 GeV (solid lines) and 100 GeV (dashed lines). Indicated as "slow" are the curves obtained in the slow WIMP–halo scenario. The others use the fast WIMP–halo. As can be seen, for heavier WIMPs the effect of detuning from the optimum, here the maxima of the curves, is small. The effect for light WIMPs is shown in the text

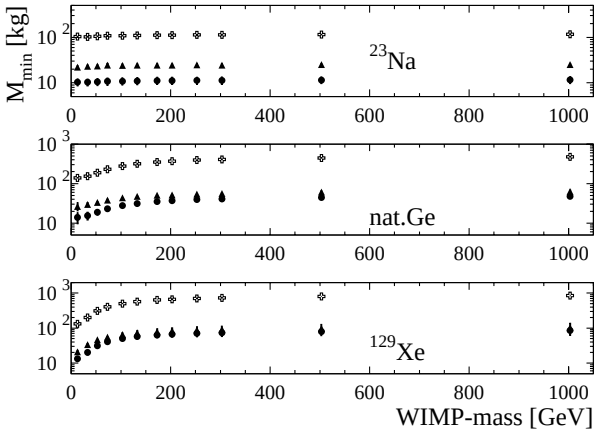

Fig. 4. Minimum target mass needed for a direct detection experiment to detect modulations as the WIMP signature as function of the WIMP mass in GeV (dots). The assumptions in this picture are a zero background rate $\langle B\rangle = 0$ and an optimistic WIMP candidate rate of $R_{\rm expect} = 1$ cpd/kg ($N\,P = 365$ days; 97.5% C.L.). To change the assumptions and results use the scaling relation given in the text. The range of minimum masses is due to halo velocity variations. The change in these ranges is a form factor effect which depends on the target nucleus mass. Changes due to a 10^3 cpd background (triangles) and due to an expected rate of 0.1 cpd/kg (crosses) are also shown

Using (for $\langle B\rangle = 0$) [5, 3.10]:

$$\langle S_{min}(E)\rangle = \frac{2\,\langle R\rangle^2}{N\cdot P}\,\frac{1}{\delta^2(E)}\;, \qquad (7)$$

where P is the number of days, N the number of years and $\langle R\rangle = 2\,r_0$ (4), one can evaluate the optimum recoil energy threshold by minimizing the mass–sensitivity

$$s = 1/(\delta^2\,\gamma)\;, \qquad (8)$$

as function of the threshold (see Fig. 3).

Figure 2 shows normalized WIMP–spectra γ(E)/dE for a 60 GeV WIMP scattered on ^{23}Na nuclei in the fast (top) and the slow (bottom) halo scenario. These curves show the generic shape of the signal, independent from cross sections or WIMP–halo densities. In Fig. 3 one can study for the examples of a light (30 GeV) and heavier (100 GeV) WIMP the effect of detuning the detector from the optimum. For heavier WIMPs the effect is small (order 100 g higher minimum mass). For the light WIMP, minimum masses increase as follows for three more realistic thresholds (slow halo scenario): For a NaI detector with 5 keV threshold (≈15 keV recoil energy) mass bounds raise from 8.6 kg (at optimum) to 9.6 kg. For a Germanium detector with 5 keV threshold (≈ 20 keV) from 11.9 kg to 18.4 kg and for a Xenon detector (12 keV) from 16.9 kg to 27.3 kg. Detuning from the optimum always worsens the mass bounds.

Regarding the analysis scheme we point out as another result that we found spectrum modulations, i.e. modulation of small energy regions of the order of some keV as a typical detector resolution, disfavored compared to integral count rate modulations. Although the amplitude *delta* can reach high values above 10% for selected energy regions of a WIMP–spectrum (dependent on the WIMP–mass) the gain is lost because of the low signal as shown for example in Fig. 2. The minimum masses raise on average by a factor ten so this is not a minor effect. Experiments analyzing a single, broad energy bin, starting at about the optimum thresholds (WIMP–mass dependent) will be able to find the WIMP signature long before an experiment looking for modulation of small energy bins.

A second analysis scheme mentioned in the literature is to correlate at least two energy bins containing the maximum and minimum WIMP counts twice a year [2]. Note that this is nothing else then what the transformation in eqn. (2) accomplishes. Every other way of 'correlating' the max. and min. containing bins, e.g. subtracting them, is worse since it is not signature specific like (2). As one knows the frequency and phase of the modulation, application of this knowledge via (2) yields the best analysis procedure.

Our results for the minimum mass are shown in Fig. 4 and the calculated values for E^{thr}_{opt} are summarized in Tab. 1. Note that in case of ionization detectors these threshold recoil energies first have to be scaled by the ionization efficiency for the specific target material used in an existing or planned experiment to obtain the electron equivalent energies [1,2].

Form factors for heavy WIMPs broaden substantially the optimum recoil energy region but, as shown in Tab. 1, there remains a threshold at low recoil energy (idealized as zero keV) which produces the minimum mass bound. For heavy WIMPs a form factor produces an almost velocity independent recoil spectrum, thus an almost flat modulation amplitude for increasing recoil energies and therefore a broad optimum recoil energy region. Therefore it turns out that the most favorable recoil threshold energy is as

Table 2. The linear fit parameters ($\delta(x) = a + b\,x$) to obtain the relative modulation amplitude $\delta(E_{thr})$ as function of recoil threshold energy. The separated values correspond to $\langle v^2\rangle^{1/2} = 246(323)$ km/s, respectively. The valid recoil energy region for the fit is for ^{23}Na: 0-100 keV, nat. Ge: 0-80 keV and ^{129}Xe: 0-30 keV. For $m_W = 10$ GeV the valid recoil energy region for all target masses is 0-10 keV

	^{23}Na		nat.Ge		^{129}Xe	
m_W[GeV]	a [%]	b [%/keV]	a [%]	b [%/keV]	a [%]	b [%/keV]
10	7.7;7.3	1.20;0.69	5.2;5.8	2.36;1.35	2.3;3.5	3.70;2.30
30	9.3;8.0	0.350;0.208	7.9;6.8	0.410;0.234	6.3;5.8	0.570;0.300
50	9.4;8.0	0.246;0.144	7.1;6.2	0.220;0.120	5.1;5.0	0.280;0.150
70	9.3;8.0	0.207;0.118	6.4;5.8	0.160;0.084	4.3;4.5	0.190;0.106
100	9.3;8.0	0.181;0.102	5.7;5.3	0.120;0.062	3.7;4.2	0.140;0.078
130	9.2;8.0	0.167;0.093	5.3;5.1	0.100;0.052	3.4;4.0	0.120;0.064
170	9.2;8.0	0.157;0.087	5.0;4.9	0.086;0.046	3.2;3.9	0.100;0.054
200	9.2;8.0	0.152;0.084	4.8;4.8	0.080;0.042	3.1;3.9	0.090;0.049
250	9.1;8.0	0.147;0.081	4.6;4.7	0.073;0.039	3.0;3.8	0.081;0.044
300	9.1;7.9	0.143;0.079	4.5;4.6	0.069;0.037	2.9;3.8	0.074;0.040
500	9.1;7.9	0.136;0.075	4.2;4.5	0.060;0.033	2.8;3.7	0.062;0.033
1000	9.1;7.9	0.131;0.071	4.0;4.4	0.055;0.030	2.7;3.7	0.053;0.028

low as possible (zero keV, maximum signal). For heavy WIMPs the mass bounds in Fig. 4 become flat independent of the target material.

We choose WIMP candidate masses m_W ranging from 10 to 1000 GeV and three representative target materials as examples for low, medium and high mass nuclei (^{23}Na, nat. Ge, and ^{129}Xe). We have checked other popular target materials with similar mass numbers, *e.g.* ^{19}F, but the deviations from the example nuclei results (here from ^{23}Na) are small. The range of minimum masses due to variation of the dispersion velocity of WIMPs in the halo is smaller than the symbol sizes in Fig. 4. Note that we always use ratios of calculated WIMP spectra or rates so that we do not need to consider constant factors, *e.g.* the local halo density.

Since the results in Fig. 4 are obtained with quite unrealistic initial values like a zero background rate $\langle B\rangle = 0$ cpd and an optimistic WIMP candidate rate of $R_{\rm expect} = 1$ cpd/kg ($N\,P = 365$ days; 97.5% C.L.), we give a relation with which the results of Fig. 4 can be scaled appropriately:

$$\left(\frac{\rm m}{\rm kg}\right) = \frac{1}{2}\left(\frac{\rm M_{min}}{\rm kg}\right) \times \left(\frac{\langle R\rangle}{4}\right)^2 \times \left(\frac{365\,\rm d}{N\cdot P}\right) \times \left(1 + \sqrt{1 + 2\left(\frac{N\cdot P}{365\,\rm d}\right)\left(\frac{4}{\langle R\rangle}\right)^2 \delta^2 \times \left(\frac{\langle B\rangle}{\rm cpd}\right)}\right) \times \left(\frac{1\,\rm cpd/kg}{R_{\rm expect}}\right). \quad (9)$$

In a certain recoil energy region the relative modulation amplitude δ shows a strict linear rise as function of the recoil threshold energy. We fitted the curves in the valid energy region according to $\delta(x) = a + b\,x$ and tabulated the parameters a and b in Tab. 2. Our results now can be used to either guide the design of a new experiment or to examine, for example, allowed background rates for a fixed total WIMP rate in an existing experiment.

In Fig. 4 we included the effects of lowering the WIMP–rate expectation and introduction of an integral, flat background of 10^3 cpd. The influence of WIMP–rate expectations clearly dominates as can also be seen from 9. Using a conventional WIMP dark matter detector one is forced to build high–mass experiments of the order 1 ton or higher to reach an interesting significance level in a reasonable time. Two such proposals have appeared so far, one for a one ton NaI scintillator experiment [16] and the second for a one ton Germanium experiment, the GENIUS proposal [17,18]. Explicit experimental problems for the detection of the modulation, e.g. in the mentioned future experiments, like stability requirements for the detector response or determination of possible time–dependent background contributions (muon flux, for example) always worsen the limitations which we worked out above.

4 Conclusion

We conclude that the statistical limitations of the proposed modulation search in direct detection experiments are restrictive. The mass ranges shown in Fig. 4, however, are not unrealistic even if they have to be scaled up, for instance by a factor of one hundred.

We would like to thank V. Berezinsky for the suggestion of reference [10] and G. Garvey for valuable comments.

References

1. P.F. Smith and J.D. Lewin, Phys. Rep. **187** (1990) 203
2. R. Bernabei, Riv. Nuov. Cim. **18** (1995) 1
3. J.D. Lewin and P.F. Smith, Astrop. Phys. **6** (1996) 87
4. A. Drukier, K. Freese and D. Spergel, Phys. Rev. **D33** (1986) 3495

5. K. Freese, J. Frieman and A. Gould, Phys. Rev. **D37** (1988) 3388
6. D.N. Spergel, Phys. Rev D37 (1988) 1353; J.I. Collar and F.T. Avignone, Phys. Lett. **B275** (1992) 181; Astrop. Phys. **3** (1995) 37
7. C.J. Martoff, A. Garzella, M. Getaneh, E. Kaczanowicz, E. Neuhauser and D. Snowden-Ifft, Phys. Rev. Lett. **76** (1996) 4882
8. K. Griest, Phys. Rev. **D37** (1988) 2703
9. R. Bernabei *et.al.*, Phys. Lett. **B 389** (1997) 757; R. Bernabei et al., Preprint astro–ph/9710290; R. Bernabei *et.al.*, preprint ROM2F/97/33 - August 1st, 1997; P. Belli, talk at TAUP97, Gran Sasso Laboratory, September 7-11, 1997
10. J. Rich, Astrop. Phys. **4** (1996) 387
11. D.A. Lewis, in *Statistical methods for physical science*, eds. J.L. Stanford and S.B. Vardeman (Vol. 28, Methods of experimental physics, Academic Press, San Diego, 1994)
12. V. Bednyakov, S. Kovalenko, H.V. Klapdor–Kleingrothaus and Y. Ramachers, Z. Phys. **A357** (1997) 339; V. Bednyakov, S. Kovalenko and H.V. Klapdor–Kleingrothaus, Phys. Rev. **D55** (1997) 503
13. K. Kuijken and J. Dubinski, MNRAS **277** (1995) 1341
14. J. Engel, Phys. Lett **B264** (1991) 114
15. L. Baudis, J. Hellmig, G. Heusser, M. Hirsch, H.V. Klapdor–Kleingrothaus, S. Kolb, B. Majorovits, H. Päs, Y. Ramachers and H. Strecker, submitted to Phys. Rev. Lett.
16. R. Bernabei *et.al.*, Astropart. Phys. **4** (1995) 45
17. H.V. Klapdor–Kleingrothaus, in Proc. BEYOND THE DESERT, Castle Ringberg, Germany, June 1997 (IOP Bristol, 1998) p. 485; J. Hellmig and H.V. Klapdor–Kleingrothaus, Z. Phys. **A359** (1997) 351; H.V. Klapdor–Kleingrothaus and M. Hirsch, Z. Phys. **A359** (1997) 361; H.V. Klapdor–Kleingrothaus, J. Hellmig and M. Hirsch, J. Phys. G **24** (1998) 483
18. H.V. Klapdor–Kleingrothaus and Y. Ramachers, in *Proc. Beyond the desert: Accelerator and Non–accelerator approaches*, edited by H.V. Klapdor–Kleingrothaus and H. Päs (IOP, Bristol 1998)